Spherical indentation of a finite poroelastic coating

M. Galli and M. L. Oyen[a)]
Engineering Department, Cambridge University, Trumpington Street, Cambridge CB2 1PZ, United Kingdom

(Received 24 April 2008; accepted 17 June 2008; published online 23 July 2008)

Indentation testing of a finite poroelastic layer is considered. Finite element modeling was used to investigate spherical contact creep tests, with emphasis on the influence of layer thickness and of finite rise time on the time-dependent deformation. Thin layers are stiffened by the substrate constraint even at very small relative indenter penetrations and reach steady state more quickly than thick layers. The degree of consolidation following loading is affected by the interaction of layer thickness and rise time and cannot be predicted from either alone. These results provide guidance for micro- and nanoindentation testings of hydrogel coatings for biomedical applications. © *2008 American Institute of Physics*. [DOI: 10.1063/1.2957993]

Hydrogel coatings are being developed to improve the biocompatibility of medical implants such as catheters[1] and glucose sensors.[2] However, the greatest limitation in hydrogel use is their poor mechanical performance.[3] Although techniques are available for mechanical characterization of bulk hydrogels, such as compression or confined compression utilizing a porous platen, thin coating materials can prove difficult to test. This obstacle has been overcome in thin films on substrates in microelectronics applications, using nanoindentation testing and analysis. The basic contact mechanics principles concerned with elastic indentation of a thin layer have been considered in depth[4,5] but would not be directly applicable to a hydrated gel material exhibiting time-dependent deformation due to fluid flow. Poroelastic indentation has been considered previously for flat-punch[6] and membrane deformation[7] problems but the interactions between layer thickness and flow characteristics have not been investigated thoroughly. Previous asymptotic analysis by Athesian *et al.*[8] only considered the step-loading case; Barry and Holmes[9] also considered an asymptotic analysis in which emphasis was on an impermeable surface. The results by Barry and Holmes are intriguing, indicating a change in primary fluid direction between short and long time limits, but their analysis is not applicable to a time scale often utilized in experimental work.

As there is no closed-form analytical solution to this class of problems[10] finite element (FE) modeling is performed. The computational work is carried out using ABAQUS FE code.[11] An axisymmetric model is developed, in which the indenter is modeled as analytical rigid surface and the layer as linear poroelastic material (eight-node elements with biquadratic displacement interpolation, bilinear pore pressure interpolation, and reduced integration were adopted). Frictionless contact is imposed between the indenter and the layer surface. It is assumed that the liquid can diffuse freely across the entire layer surface, including the contact region. Note that assuming an impermeable contact region would not influence significantly the indenter response[12] and implies a much larger computational cost. The layer is considered to lie on a rigid and impervious substrate. The model geometry is determined by the nondimensional parameter

$$L^* = \frac{L}{R}, \tag{1}$$

where L is the layer thickness and R the indenter radius. The values $L^*=0.05, 0.1, 0.25, 1.0, 2.5, 5$ are considered; a schematic of the model relative dimensions is reported in Fig. 1. The modeled region is sufficiently large in radial direction for the decay in displacement and pressure fields far from the indenter be caught.

The layer is assumed to be a saturated isotropic linearly elastic porous material, whose constitutive behavior is characterized in terms of shear modulus G and Poisson's ratio ν. Here, two extreme values $\nu=0$ and $\nu=0.45$ are considered. The liquid is incompressible and its flow through the elastic skeleton depends on the permeability κ according to Darcy's law.[10]

Indentation tests are simulated under load control according to a ramp-hold profile[13] with a ramp time t_R and a load P. The rise time is characterized by the nondimensional parameter

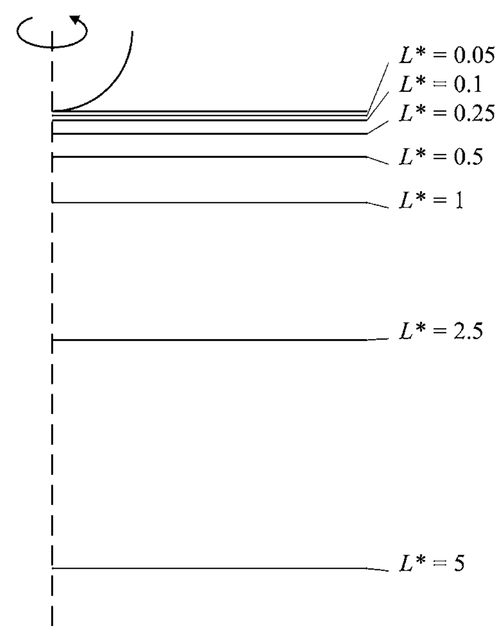

FIG. 1. Schematic of the layer thickness (L) with respect to the indenter radius (R) for values of the nondimensional film thickness L^* considered in the study.

[a)]Electronic mail: mlo29@cam.ac.uk.

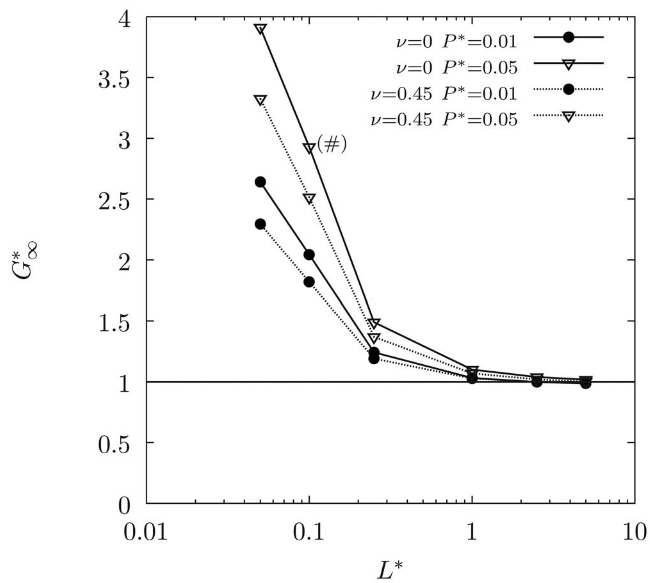

FIG. 2. Influence of the relative layer thickness (L^*) on the apparent shear modulus at infinite time (G^*_∞), computed according to Eq (5). For a layer thickness smaller than the indenter radius ($L^* < 1$) the analytical solution overestimates the the material stiffness. Note that for the data points at marked with "#" ($L^*=0.1$) the half-space approximation leads to an average error of 25% on G^*_∞ although the relative indenter penetration always complies the condition ($h/L < 0.1$), with values (from top to bottom) of $\approx 0.07, 0.06, 0.03, 0.02$.

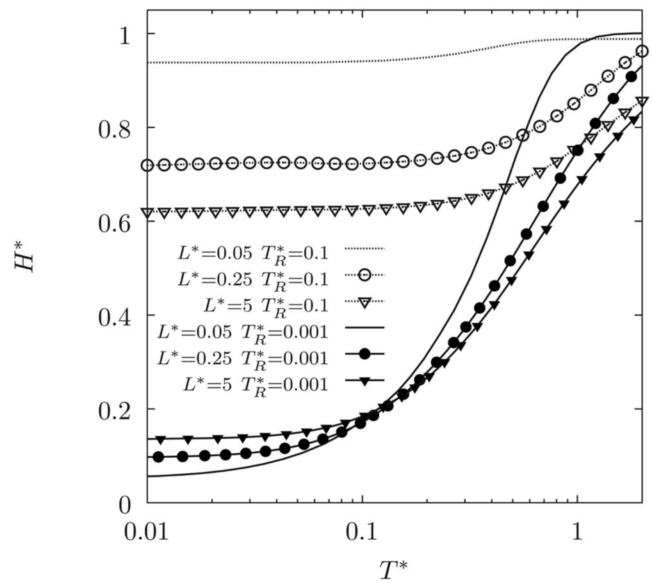

FIG. 3. Nondimensional time-displacement curves (T^*-H^*) for the minimum and maximum considered values the rise time ($T^*_R=0.001, 0.1$), three different film thicknesses ($L^*=0.05, 0.25, 5$), load magnitude $P^*=0.05$, and Poisson's ratio $\nu=0$. For the largest rise time the thinnest film develops almost all the deformation during the ramp segment of the load profile. The opposite is true for small rise-times, for which the consolidation in the thinnest films is limited. As T^* increases the influence of the rise time decreases and for $T^* > 1$ the difference between curves with different T^*_R but the same layer thickness becomes negligible.

$$T^*_R = \sqrt{\frac{G\kappa t_R}{R^2}}. \tag{2}$$

The load magnitude is defined by the nondimensional parameter

$$P^* = \frac{P}{GR^2}. \tag{3}$$

The following values are included in simulations for each layer thickness L^*: $T^*_R=0.1, 0.01, 0.001$ and $P^*=0.01, 0.05$.

Consistent with elastic thin film mechanics,[4] a thin poroelastic layer appears less compliant than a thick layer, and a thick layer can be approximated as a half space for large values of L^*. To illustrate this effect, the ratio G^*_∞ was computed

$$G^*_\infty = \frac{G^{\text{app}}_\infty}{G}, \tag{4}$$

where G^{app}_∞ is the apparent shear modulus at infinite time, computed by solving the elastic Hertzian contact expression[14]

$$h = \left(\frac{9P^2(1-\nu)^2}{64RG^2}\right)^{1/3}, \tag{5}$$

with respect to G for $h=h_\infty$. The evolution of G^*_∞ as a function of L^* is shown in Fig. 2. It can be noted how the stiffening of the response is sharply increased for thin coatings, for $L^* < 0.25$. The error in assuming a half-space condition is large for small relative indenter penetrations h/L, such that an overestimation of elastic modulus by more than a factor of 2 would occur at relative penetration depths much less than 0.1. For $L^* \geqslant 1$ the layer can be considered a half space and the FE solution compares well with the analytical solution for an elastic half space. Further results of the simulations are presented in terms of a degree of consolidation H^*, as proposed by Agbezuge and and co-worker,[12,15]

$$H^* = \frac{h(t) - h_0}{h_\infty - h_0}, \tag{6}$$

where $h(t)$ is the time-dependent rigid displacement of the indenter, h_0 is the instantaneous displacement in case of step loading, and h_∞ is the ultimate value. Since the extreme values of the displacement are independent of the transient poroelastic response, they are assessed by means of purely elastic simulations, with $\nu=0.5$ for h_0 and $\nu=0, 0.45$ for the respective values of h_∞. Further, a nondimensional time parameter T^* is defined for ramp loading as a modification of that used previously for step loading,[12,15]

$$T^* = \sqrt{\frac{2G\kappa(t-t_R)}{Rh(t)}}. \tag{7}$$

The present parametric study allows assessment of the interaction between layer thickness and rise time. The results for some key combinations of the L^* and T^*_R values are summarized in Fig. 3. The substrate has a twofold effect on the time-dependent deformation: on one hand it promotes a quicker rise in the hydrostatic pressure, therefore a higher fluid flux beneath the indenter (faster consolidation), on the other hand, given its imperviousness, the substrate constrains the diffusion process (slower consolidation). The effects of these competing mechanisms are evident in Fig. 3: for larger rise times ($T^*_R=0.1$) the rise in hydrostatic pressure prevails and the amount of consolidation developed during the ramp is much larger for thinner layers. For shorter rise times ($T^*_R=0.001$) the trend is opposite and the substrate constraint to flow minimizes consolidation. In both cases, as time increases following the ramp, the first mechanism prevails and the system approaches steady state substantially faster in thinner layers. This results in the curves for $T_R^*=0.001$ crossing over at $T^* \approx 0.15$. These results, demonstrating a strong interaction of coating thickness and transient response, have major implications from an experimental point of view: if comparing coatings of different thicknesses it is critical to know how the rise time compares to the material intrinsic time response, but it is unclear that this could be known *a priori*. Of course, a sufficiently short load ramp is required to capture a material's transient response, although this might be beyond the capabilities of the instrument being used.

For a half-space and step-loading conditions, by adopting the nondimensional parameters T^* and H^* it is possible to build master curves which represent the test response as a function of the test profile (T_R^*) and of the material properties (G, ν, and κ),[12,15] Given the experimental data [$h(t)$ and possibly one or both h_0 and h_∞], by fitting them to the appropriate master curve it is possible to identify the elastic properties and the permeability of the material, as suggested by Oyen.[16] Such an approach can be extended to form a library of master curves for varying T_R^*, P^*, and L^*. With this library, material parameter identification can be conducted without the need for inverse FE analysis, allowing for rapid analysis of large numbers of indentation tests. Moreover, when the material behavior cannot be approximated as linear poroelastic, this first identification can represent the starting point for subsequent FE modeling which includes more complex constitutive laws.

M. Galli was supported by Grant No. PBELB-120953 from the Swiss National Science Foundation.

[1] S. H. Yang, Y. S. Lee, F. H. Lin, J. M. Yang, and K. S. Chen, J. Biomed. Mater. Res., Part B: Appl. Biomater. **83**, 304 (2007).
[2] B. Yu, C. Wang, Y. M. Ju, L. West, J. Harmon, Y. Moussy, and Y. F. Moussy, Biosens. Bioelectron. **23**, 1278 (2008).
[3] J. A. Burdick and M. M. Stevens, *Biomedical Hydrogels*, in *Biomaterials, Artificial Organs, and Tissue Engineering* (Woodhead, Cambridge, 2005).
[4] H. Gao, C. Chiu, and J. Lee, Int. J. Solids Struct. **29**, 2471 (1992).
[5] M. J. Matthewson, J. Mech. Phys. Solids **29**, 89 (1981).
[6] V. C. Mow, M. C. Gibbs, W. M. Lai, W. B. Zhu, and K. A. Athanasiou, J. Biomech. **22**, 853 (1989).
[7] X. Chen, A. C. Dunn, W. G. Sawyer, and M. Sarntinoranont, J. Biomech. Eng. **129**, 156 (2007).
[8] G. A. Athesian, W. M. Lai, W. B. Zhu, and V. C. Mow, J. Biomech. **27**, 1347 (1994).
[9] S. I. Barry and M. Holmes, J. Appl. Math. **66**, 175 (2001).
[10] H. F. Wang, *Theory of Linear Poroelasticity with Applications to Geomechanics and Hydrogeology* (Princeton University Press, New Jersey, 2000).
[11] ABAQUS Version 6.7, SIMULIA.
[12] L. K. Agbezuge and H. Deresiewicz, Isr. J. Technol. **12**, 322 (1974).
[13] A. K. Bembey, A. J. Bushby, A. Boyde, V. L. Ferguson, and M. L. Oyen, J. Mater. Res. **21**, 1962 (2006).
[14] K. L. Johnson, *Contact Mechanics* (Cambridge University Press, Cambridge, 2004).
[15] H. Deresiewicz, Isr. J. Technol. **15**, 89 (1977).
[16] M. L. Oyen, J. Mater. Res. **23**, 1307 (2008).